

Maxim A. Zapara · Nikolay D. Tutyshkin ·  
Wolfgang H. Müller · Kerstin Weinberg · Ralf Wille

## A physico-mechanical approach to modeling of metal forming processes—part I: theoretical framework

Received: 10 October 2007 / Accepted: 29 April 2008 / Published online: 8 August 2008  
© Springer-Verlag 2008

**Abstract** A combined physico-mechanical approach to research and modeling of forming processes for metals with predictable properties is developed. The constitutive equations describing large plastic deformations under complex loading are based on both plastic flow theory and continuum damage mechanics. The model which is developed in order to study strongly plastically deformed materials represents their mechanical behavior by taking micro-structural damage induced by strain micro-defects into account. The symmetric second-rank order tensor of damage is applied for the estimation of the material damage connected with volume, shape, and orientation of micro-defects. The definition offered for this tensor is physically motivated since its hydrostatic and deviatoric parts describe the evolution of damage connected with a change in volume and shape of micro-defects, respectively. Such a representation of damage kinetics allows us to use two integral measures for the calculation of damage in deformed materials. The first measure determines plastic dilatation related to an increase in void volume. A critical amount of plastic dilatation enables a quantitative assessment of the risk of fracture of the deformed metal. By means of an experimental analysis we can determine the function of plastic dilatation which depends on the strain accumulated by material particles under various stress and temperature-rate conditions of forming. The second measure accounts for the deviatoric strain of voids which is connected with a change in their shape. The critical deformation of ellipsoidal voids corresponds to their intense coalescence and to formation of large cavernous defects. These two damage measures are important for the prediction of the meso-structure quality of metalware produced by metal forming techniques. Experimental results of various previous investigations are used during modeling of the damage process.

**Keywords** Plasticity · Continuum damage mechanics · Metal fracture · Plastic flow · Damage kinetics · Deformation · Stress · Temperature · Micro-structure · Strain micro-defect · Void · Modeling · Constitutive equation

**PACS** 46.35.+z · 81.40.Lm · 61.72.Qq · 46.50.+a · 62.20.mm

---

Communicated by S. Roux

---

M. A. Zapara · N. D. Tutyshkin  
Department of Technological Mechanics, Tula State University, 300600 Tula, Russia

W. H. Müller (✉) · R. Wille  
Institut für Mechanik-LKM, Technische Universität Berlin, Sekretariat MS 02,  
Einsteinufer 5, 10587 Berlin, Germany  
E-mail: Wolfgang.H.Mueller@tu-berlin.de

K. Weinberg  
Institut für Mechanik und Regelungstechnik - Mechatronik, AG Festkörpermechanik, Universität Siegen,  
Paul-Bonatz-Straße 9-11, 57076 Siegen, Germany

## 1 Introduction

Many technological processes of metalware production are based on the combination of forming operations (deformation processing) and heat treatment. The operating characteristics of finished products are substantially defined by the mechanical and micro-structural properties of the materials. A leading role in the technological creation of optimized mechanical and micro-structural properties of the materials of finished products is played by forming operations. Using models of metal forming processes successfully helps solving problems appearing during development of state-of-the-art production techniques.

A combined physico-mechanical approach based on the study of both mechanical and micro-structural properties amounting to important technological parameters of strained metals is developed for the analysis of forming processes. This approach is founded on advanced methods of plasticity theory which include physico-mechanical models of strained materials, methods for calculation of associated stress and strain rate fields, and methods for determination of mechanical and micro-structural parameters related to technological and operational characteristics of finished components.

It should be noted that the mathematical and the applied theory of plasticity was developed based on conceptual aspects of continuum mechanics. Basic equations and models in classical plasticity theory [15] describe a mechanical behavior of deformed solids without taking their micro-structural properties (i.e., parameters of the meso-structure, such as void growth and coalescence, polycrystalline unit grain size, volume fraction of heterogeneous phases, internal energy of hardening, healing of meso-defects at elevated strain temperatures, etc.) into consideration. The mechanical characteristics of materials depend on deformation process parameters (e.g., strain extent, rate, and temperature; stress-strain state) and they are determined on the basis of macro-experiments for macro-samples [17]. Mechanisms of micro-structural behavior of deformed materials are not studied in macro-experiments.

Investigations in the field of technological mechanics have shown that operational properties of machine components (e.g., the ability to withstand high strain rates or intense thermal and physico-chemical loads) depend not only on macro-mechanical but also micro-structural characteristics of their materials. In this context there is a necessity for the development of a combined physico-mechanical approach to an understanding and modeling of deformation processes of materials. The model for deformed materials should describe their mechanical behavior taking micro-structural characteristics (e.g., damage by strain micro-defects) into consideration. The formulation of the models as well as defining constitutive equations for deformed and damaged materials with predictable micro-structural and mechanical properties require complex experimental studies of the material characteristics depending on the parameters of the deformation processes.

In the publications dedicated to a comprehensive physico-mechanical approach similar to the one presented in this paper great attention is given

- to the development of a theory of elastic-viscoplastic deformations of crystalline solids (e.g., [4,24,38]);
- to studies on meso-structural levels of deformation (e.g., [13,29]);
- to a methodology of the underlying physics in continuum mechanics terms as a construction base for material models with meso-structural properties (e.g., [1,8]);

Less attention is given to the development of the theory of plastic flow of solids when subjected to large finite strains under complex loading together with a meso-mechanical approach to damage, i.e., effect of grain size, dislocation ensembles, coalescence of voids, etc.

The theory of polycrystal plastic flow finds an application for research and modeling of metal forming procedures where target properties develop under large finite strains. The use of plastic flow theory is of particular current interest for an understanding of the processes during three-axial deformation with strong variation of stress conditions both in time and within the plastically deformed regions. The combined use of plastic flow theory and basic concepts of continuum damage mechanics allows us to study the change of the ductile properties of processed materials during deformation in view of many factors including nucleation, propagation, growth, coalescence, and possible healing of strain micro-defects. This analysis enables one to predict accurately the strain damage for deformed materials. It is essential when manufacturing metalware to be used under high and intense loads.

Such combined methods were developed in some previous works. Kolmogorov et al. [21] and Bogatov [3] studied the processes of rolling, dragging, and drawing of metallurgical blanks and predicted the corresponding strain damage. Gelin [12] presented finite element models of damage for bulk and sheet metal forming processes. Tang et al. [33] used a tensor measure of damage for predicting the material fracture during sheet metal stamping. Xiang and Wu [39] analyzed and simulated superplastic forming of Al-alloys using a void

damage criterion. Pironi et al. [30] predicted fracture of low-alloy steels subjected to cyclic plastic loading on the basis of continuum damage mechanics models. On the basis of both plastic flow theory and dissipative damage mechanics Makarov et al. [26] studied isothermal super-plastic extrusion of solid shapes made of carbon steels (C: 0.75–1.75%).

In the present work the authors use an integrated approach for research and modeling of plastic deformation of metals subjected to complex loading. It is based on plastic flow theory and tensor theory of strain damage. This approach involves determination of consistent stress and plastic flow velocity fields under complex loading conditions using enhanced models of processed materials. It is particularly appropriate for the analysis and design of non-stationary and high-speed forming processes with strong variation of stress and strain rate conditions.

The modeling of deformation processes for materials with predictable structural and mechanical properties is based on the fundamental equations of continuum mechanics, rheological correlations to describe the properties of solids depending on the deformation, and on experimental data for the formulation of boundary conditions in arising problems of plasticity theory.

## 2 Basic equations of metal plastic flow

Plastic strains in deformed metals amount to 70–90% being  $\approx 10^2$  larger than elastic strains in metal forming processes (e.g., drawing, die forging, extrusion). Thus, the deformed material is considered as a rigid-plastic solid whose yield strength depends on strain, strain rate, and temperature, as well as the parameters of the mesoscopic structure. The calculation of stress-strain state and related parameters of forming processes by using the model of rigid-plastic solids leads to quite satisfactory results corresponding to experimental data. The evolution of strain damage results in plastic dilatation. According to test data plastic dilatation of engineering materials does not exceed 2–5% even at large processing deformations. This fact enables one to make an assumption concerning the materials incompressibility when determining the fields of plastic flow velocities.

The equations relevant for a description of plastic flow of solids (in orthogonal curvilinear coordinates  $x^i$ ,  $i = 1, 2, 3$ ) are:

- equilibrium of forces ( $\nabla_j$  covariant differentiation;  $\sigma^{ij}$  contravariant components of the stress tensor;  $\rho$  density of the material;  $a^i$ ,  $F^i$  contravariant components of acceleration and external force density, respectively):

$$\nabla_j \sigma^{ij} = \rho (a^i - F^i), \quad (1)$$

- incompressibility condition ( $v^i$  contravariant components of velocity):

$$\nabla_i v^i = 0, \quad (2)$$

- yield condition ( $e_{ij}$  covariant components of the deviatoric strain;  $T$  thermodynamic temperature;  $\chi_s$  parameters related to the local deformation by nonholonomic correlations;  $\mu_k$  physico-structural parameters):

$$f(s^{ij}, e_{ij}, T, \chi_s, \mu_k) = 0, \quad (3)$$

- associated flow rule ( $\dot{\lambda}$  a positive scalar proportional to plastic strain force;  $s^{ij}$  contravariant stress deviator components;  $t$  time;  $\dot{e}_{ij}$  covariant components of the deviatoric strain rate):

$$\dot{e}_{ij} = \dot{\lambda} \frac{\partial f}{\partial s^{ij}}, \quad (4)$$

- rate equations for the physico-structural parameters:

$$\frac{d\mu_k}{dt} = \dot{\mu}_k (s^{ij}, e^{ij}, T, \chi_s, \mu_k). \quad (5)$$

More explicitly we may write ( $\Gamma_{kj}^i$  denote the Christoffel symbols, cf., [22]):

$$\begin{aligned}\nabla_j \sigma^{ij} &= \frac{\partial \sigma^{ij}}{\partial x^j} + \sigma^{kj} \Gamma_{kj}^i + \sigma^{ik} \Gamma_{kj}^j, \\ \nabla_i v^i &= \frac{\partial v^i}{\partial x^i} + v^k \Gamma_{ik}^i, \quad a^i = \frac{\partial v^i}{\partial t} + v^j \left( \frac{\partial v^i}{\partial x^j} + v^k \Gamma_{kj}^i \right), \\ \dot{e}_{ij} &= \frac{1}{2} \left( \frac{\partial v_i}{\partial x^j} + \frac{\partial v_j}{\partial x^i} - 2v_k \Gamma_{ij}^k \right).\end{aligned}\quad (6)$$

For orthogonal coordinates the non-vanishing Christoffel symbols can be calculated with the following formulae ( $H_i$  are parameters related to the metric tensor,  $g_{ij}$ , namely  $H_i = \sqrt{g_{ii}}$ ):

$$\Gamma_{ij}^i = \frac{1}{H_i} \frac{\partial H_i}{\partial x^j}, \quad \Gamma_{jj}^i = -\frac{H_j}{H_i^2} \frac{\partial H_j}{\partial x^i}.\quad (7)$$

The six equations shown in (4) are not mutually independent. They can be reduced to three so-called coaxiality equations for the deviators of the strain rate and of the stresses (i.e., coincidence of their principal axes):

$$\frac{\dot{e}_{ij}}{\sigma_{ij}} = \frac{\dot{e}_{ii} - \dot{e}_{jj}}{\sigma_{ii} - \sigma_{jj}} \equiv \frac{\dot{e}_{ii} - \dot{e}_{jj}}{s_{ii} - s_{jj}}, \quad i, j = 1, 2, 3, \quad i \neq j\quad (8)$$

and a condition of similarity between these deviators

$$\phi_{\dot{e}} = \phi_{\sigma},\quad (9)$$

where  $\phi_{\dot{e}}$  and  $\phi_{\sigma}$  denote the deviator phase angles (Lode angles) which are defined by the following equations:

$$\cos(3\phi_{\dot{e}}) = -\frac{3\sqrt{3}I_3(\dot{e}_{ij})}{2I_2^{3/2}(\dot{e}_{ij})}, \quad \cos(3\phi_{\sigma}) = -\frac{3\sqrt{3}I_3(s_{ij})}{2I_2^{3/2}(s_{ij})},\quad (10)$$

where  $I_2(\dot{e}_{ij}) = \dot{e}^2$ ,  $I_2(s_{ij}) = s^2$ , and  $I_3(\dot{e}_{ij})$ ,  $I_3(s_{ij})$  are second and third invariants of the strain rate and stress deviators, respectively.

In what follows a yield criterion of the von Mises type will be used ( $\tau_s$  is the yield stress under shear, see also Eq. (19) below):

$$f(s^{ij}, e_{ij}, T, \chi_s, \mu_k) = \frac{1}{2} s_{:j}^i s_{:i}^j - \tau_s^2(e_{ij}, T, \chi_s, \mu_k) = 0.\quad (11)$$

For the parameters  $\chi_s$ , which are associated with the deformation, the intensity of shear strain rate,  $\dot{\Lambda}$ , and the cumulative shear strain,  $\Lambda$ , or Odquist parameter, are used:

$$\dot{\Lambda} = \sqrt{2\dot{e}_{:j}^i \dot{e}_{:i}^j}, \quad \Lambda = \int_{s(t)} \sqrt{2\dot{e}_{:j}^i \dot{e}_{:i}^j} dt,\quad (12)$$

where  $\dot{e}_{:j}^i$  denote the mixed components of the strain rate deviator. The parameters  $\dot{\Lambda}$  and  $\Lambda$  are connected by the non-holonomic equation  $d\Lambda/dt = \dot{\Lambda}$ . For each strain path,  $s(t)$ , the parameter  $\Lambda$  can be determined by integration according to Eq. (12) provided that strain rates  $\dot{e}_{:j}^i$  are known.

As physico-structural parameters  $\mu_k$  we will specifically choose a micro-defect damage parameter  $\omega$ , the grain size  $D$  of the polycrystal, and the energy characteristic  $u^{(\mu)}$  of irreversible changes of the crystal lattice (viz., a density of the internal energy of hardening,  $u_h$ ). The afore-mentioned structural properties of engineering materials have a significant influence upon the operating characteristics of finished products.

The analysis of spatial stress and velocity fields dependent on mechanical and structural properties of deformed metals is based on a solution of the combined basic Eqs. (1)–(5) using the technique of yield zone mapping in deviatoric stress space [35], which will be explained in greater detail in the second part of this paper.

### 3 Associated law of metal plastic flow

The equation for the yield surface (3) together with the flow rule (4) determine an associated law of metal plastic flow. Plastic flow of strained materials is accompanied by rate effects and a structural change that substantially affects the technological parameters and working characteristics of the final products. Rate effects, such as inertial stress, thermal flux, or rate hardening and structural changes are satisfactorily described by the yield surface (3). The flow rule (4) establishes correlations between the strain rate  $\dot{e}_{ij}$  (or the increments  $de_{ij}$ ), the strains  $e_{ij}$ , and the stresses  $s^{ij}$  for large plastic deformations.

The structure of the flow rule (4) satisfying the yield condition (3) is determined from the principle of maximum power of deformation (Hill 1948):

$$d\lambda = \dot{\lambda} dt = h d'f, \quad (13)$$

where  $h > 0$  is a function of various parameters that define the physico-mechanical conditions of the material. Moreover,  $d'f$  is the differential of the yield function ( $f = 0$ ) provided that the strain increments vanish, i.e.,  $de_{ij} = 0$ , in contrast to the total differential  $df$  of the yield function (consistency condition):

$$df = \frac{\partial f}{\partial s^{ij}} ds^{ij} + \frac{\partial f}{\partial e_{ij}} de_{ij} + \frac{\partial f}{\partial T} dT + \frac{\partial f}{\partial \chi_s} d\chi_s + \frac{\partial f}{\partial \mu_k} d\mu_k = 0. \quad (14)$$

By combination of Eqs. (4) and (13) we obtain  $de_{ij} = h \frac{\partial f}{\partial s^{ij}} d'f$ . Provided that strain increments are zero, i.e.,  $de_{ij} = 0$ , the differential of the yield surface is given by:

$$d'f = \frac{\partial f}{\partial s^{ij}} ds^{ij} + \frac{\partial f}{\partial T} d(T - \Delta T_s) + \frac{\partial f}{\partial \mu_k} d'\mu_k > 0, \quad (15)$$

where  $\Delta T_s$  is a temperature increment related to the dissipated power density  $\dot{w} = \frac{dw}{dt} = s^{ij} \dot{e}_{ij}$  ( $w$  denotes the density of the work of deformation);  $d'\mu_k$  is a differential of physico-structural parameters *not* related to the deformations  $e_{ij}$ . Note that the inequality  $d'f > 0$  implies a condition of active loading, i.e., of further continuation of plastic deformation.

From Eqs. (13)–(15) it follows that

$$\frac{d\lambda}{h} + \frac{\partial f}{\partial e_{ij}} de_{ij} + \frac{\partial f}{\partial T} d(\Delta T_s) + \frac{\partial f}{\partial \chi_s} d\chi_s + \frac{\partial f}{\partial \mu_k} (d\mu_k - d'\mu_k) = 0. \quad (16)$$

The differentials  $d(\Delta T_s)$ ,  $d\chi_s$ ,  $d\mu_k - d'\mu_k$  are related to the strain increments  $de_{ij}$  as follows:

$$d(\Delta T_s) = K_s de_{ij}, \quad d\chi_s = A_s de_{ij}, \quad d\mu_k - d'\mu_k = B_s de_{ij} \quad (17)$$

where  $K_s$ ,  $A_s$ ,  $B_s$  are functions of the physical and mechanical parameters of materials.

Equation (16) is now combined with Eq. (17) to yield:

$$\frac{d\lambda}{h} + \left( \frac{\partial f}{\partial e_{ij}} + K_s \frac{\partial f}{\partial T} + A_s \frac{\partial f}{\partial \chi_s} + B_s \frac{\partial f}{\partial \mu_k} \right) de_{ij} = 0. \quad (18)$$

By virtue of the associative flow rule (4) the scalar  $h$  can now be identified:

$$h = - \left( \frac{\partial f}{\partial e_{ij}} + K_s \frac{\partial f}{\partial T} + A_s \frac{\partial f}{\partial \chi_s} + B_s \frac{\partial f}{\partial \mu_k} \right)^{-1} \left( \frac{\partial f}{\partial s^{ij}} \right)^{-1}. \quad (19)$$

The von Mises yield function (11) will be used for finding the scalar  $d\lambda = h d'f$ . The corresponding determination procedure for this function is outlined below. Experiments have been performed and examined in order to determine the von Mises yield function (11). The experimental data indicate a strong effect of strain, temperature, strain rate, and of the material physico-structural properties on the yield point, i.e.,:

$$\sigma_s = \tau_s \sqrt{3} = \sigma_s(e_i, \dot{e}_i, T, \mu_k), \quad (20)$$

where  $e_i = \Lambda / \sqrt{3}$  denotes the equivalent strains, i.e., an *intensity* (note the index  $i$  in  $e_i$ ) of cumulative strains, and  $\dot{e}_i = \dot{\Lambda} / \sqrt{3}$  is the corresponding intensity of strain rates.

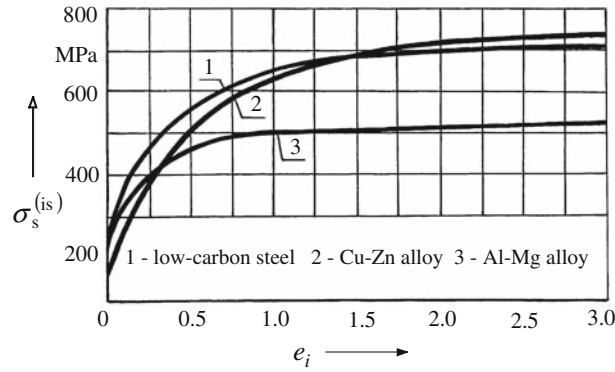


**Fig. 1** Isothermal hardening curves

The dependence (20) is represented by the hypersurface ( $f=0$ ) for each material in the space  $(\sigma_s, e_i, \dot{e}_i, T, \mu_k)$ . The hypersurface  $f=0$  can be specified for each material by means of supporting curves to be constructed by means of the experimental database for various strain conditions. Based on experimental data the following mathematical form of non-isothermal hardening curves was established:

$$\sigma_s = \sigma_s^{(is)} \exp \left[ -\alpha \left( \frac{T - T_0}{T_{\max} - T_0} \right)^q \right], \quad (21)$$

where  $\sigma_s^{(is)} = \sigma_s^{(is)}(e_i, \dot{e}_{i0}, T_0, \mu_k)$  refer to isothermal hardening curves obtained for various materials at a fixed strain rate  $\dot{e}_{i0}$  and an initial temperature  $T_0$ , cf., Fig. 1.  $T_{\max}$  is the maximum temperature of the process,  $\alpha$  and  $q$  are parameters used in the equation for the temperature dependent yield strength  $\sigma_s$ .

Uniaxial compression tests have been made on compound cylindrical specimens in order to obtain hardening curves for the investigated metals under isothermal conditions (cf., Fig. 1). Each compound specimen consisted of three identical cylindrical specimens. Plastic compression of the compound specimen allows attaining large deformations equivalent to those during metal forming processes.

The character of temperature dependence for the yield stress  $\sigma_s(T)$  can be described by a decrease in the activation energy, i.e., by a decrease in the energy threshold required for the movement of dislocations as a result of thermal fluctuations. Note that the power dependence in (21) can also be motivated from basic principles of thermodynamics for deformed metals [40,41]. The construction of non-isothermal curves for materials with changing microstructure is a rather complex problem. It becomes complicated due to the necessity to determine values  $T$ ,  $\alpha$ ,  $q$  which depend on initial conditions and on the strain path  $s$ . The change in temperature,  $T$ , relates to both the effect of thermal flux due to the deformation of the material and to the addition or removal of heat as part of the material processing.

The various parameters included in Eq. (21) are determined as follows. The dependency of the isothermal yield point on strain can be approximated by an exponential three-parameter fit:

$$\sigma_s^{(is)} = \sigma_{0.2} + B e_i^{(n_0 - n_1 e_i)}, \quad (22)$$

where  $\sigma_{0.2}$  denotes the initial yield point and  $B$ ,  $n_0$ ,  $n_1$  are strain hardening parameters which can be found by the experimental curve.

During polycrystalline deformation the initial material yield point depends on the grain size. This dependence can be physically explained as grain-to-grain strain transfer and it can be quantified by the *Hall-Petch* correlation [40]:

$$\sigma_{0.2} = \sigma_0 + k_y D^{-\frac{1}{2}}, \quad (23)$$

where  $D$  is an average grain diameter,  $\sigma_0$  characterizes a resistance of the movement of free dislocations, and  $k_y$  is a measure proportional to the stress  $\sigma_d$  required for the movement of locked dislocations and depending on the dislocation arrangement of the metal, i.e.,:

$$k_y = \sigma_d l^{\frac{1}{2}}, \quad (24)$$

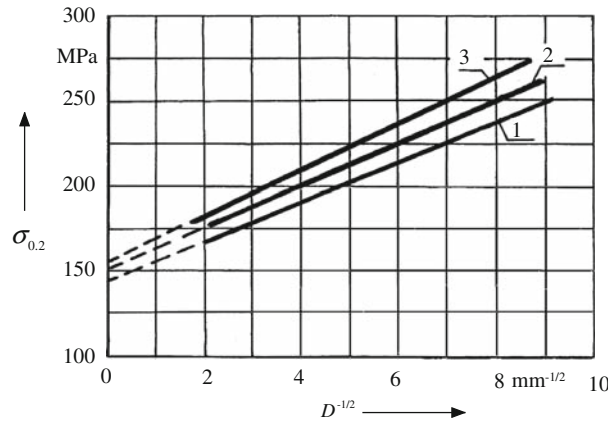


**Fig. 2** Effect of grain size  $D$  on initial yield point  $\sigma_{0.2}$  of low-carbon steel for different damage  $\omega$  (dislocation content); 1: 0.05 ( $10^7$ – $10^8$   $\text{cm}^{-2}$ ), 2: 0.25 ( $10^9$ – $10^{10}$   $\text{cm}^{-2}$ ), 3: 0.45 ( $10^{10}$   $\text{cm}^{-2}$ )

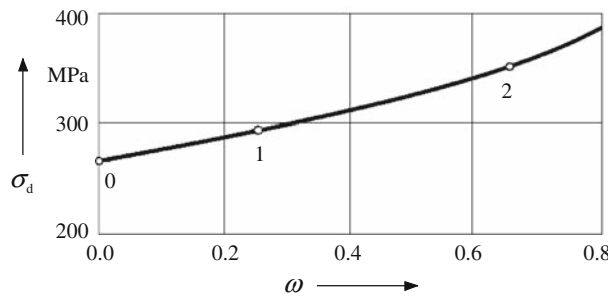


**Fig. 3** Relationship between stress  $\sigma_d$  and damage  $\omega$  during deformation of low-carbon low-alloy steel (C: 0.08–0.20 %, Cr: 0.15–0.30 %)

where  $l$  indicates an average distance between the grain boundary and the nearest dislocation source. Equation (23) is in agreement with experimental data given by Yokobori [40] and obtained during uniaxial tension of low-carbon low-alloy steel specimens (cf., Fig. 2). Its form can also be motivated by basic correlations for the dislocation content as shown by Yokobori [40]. The yield points for steels with sub-grain sizes  $D$  varying in between 0.0005 and 0.0006 mm can be found by a modified Hall-Petch correlation:

$$\sigma_{0.2} = \sigma_0 + k_y D^{-\frac{1}{2}} + k_y^* D^{-1}, \quad (25)$$

where  $k_y^*$  denotes a material constant for specified conditions which depends on the structure of sub-boundaries.

Based on experiments a relation between the stress  $\sigma_d$  required for the movement of locked dislocations and the measure  $\omega$  of damage by strain micro-defects can be established (cf., Fig. 3):

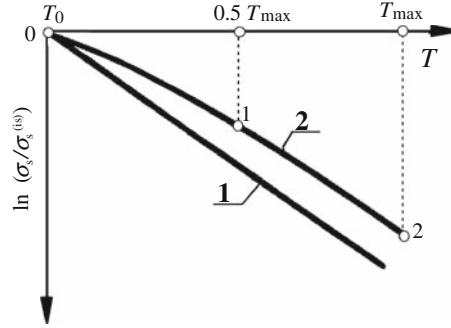
$$\sigma_d = \sigma_{d/\omega=0} + A\omega^m, \quad m = \frac{\ln \frac{\sigma_d^{(2)} - \sigma_{d/\omega=0}}{\sigma_d^{(1)} - \sigma_{d/\omega=0}}}{\ln \frac{\omega^{(2)}}{\omega^{(1)}}}, \quad A = \frac{\sigma_d^{(1)} - \sigma_{d/\omega=0}}{\omega^{(1)m}} = \frac{\sigma_d^{(2)} - \sigma_{d/\omega=0}}{\omega^{(2)m}}. \quad (26)$$

where, as indicated,  $A$  and  $m$  are material constants which have been found by three control points 0 ( $\omega = 0$ ;  $\sigma_{d/\omega=0}$ ), 1 ( $\omega^{(1)}$ ;  $\sigma_d^{(1)}$ ), and 2 ( $\omega^{(2)}$ ;  $\sigma_d^{(2)}$ ) of the empirical curve shown in Fig. 3.

In order to determine the function  $\sigma_d(\omega)$  experimentally two-stage tension tests were carried out with pre-annealed specimens made of low-carbon low-alloy steel. The damage measure,  $\omega$ , and the dislocation content,  $\rho^*$ , were quantified after each stage. The damage measure  $\omega$  was found by a technique outlined in Sect. 4.1 of the present paper. The dislocation content  $\rho^*$  was estimated on the basis of X-ray crystal analysis. Then the stress  $\sigma_d$  was calculated via the known dependence  $\sigma_d(\rho^*)$ , [40]. The experimental results obtained for the function (26) are given in Table 1.

**Table 1** Experimental parameters of the function  $\sigma_d(\omega)$  for low-carbon low-alloy steels

Stages of the deformation	Damage measure, $\omega$	Dislocation content, $\rho^*$ , $\text{cm}^{-2}$	Stress, $\sigma_d$ , MPa	Material constants	
				$A$ , MPa	$m$
Initial state (point 0)	0	$10^8$	265	157	1.40
First stage of deformation (point 1)	0.26	$10^9$	289		
Second stage of deformation (point 2)	0.66	$10^{11}$	353		

**Fig. 4** Representation of the temperature dependence (21) in the plane  $\ln(\sigma_s/\sigma_s^{(is)})$  vs.  $T$ : 1 linear relation ( $q = 1$ ), 2 allowing for physico-structural changes ( $q > 1$ )

The power law dependence of the stress  $\sigma_d$  on the damage  $\omega$  is motivated by an increase in dislocation density  $\rho^*$  during plastic flow of the material. However, for a more reliable substantiation of the relation (26) it is necessary to verify it experimentally for a number of structural metals.

Consequently, after insertion of Eqs. (23)–(26) we may write for the isothermal yield point of Eq. (22):

$$\sigma_s^{(is)} = \sigma_0 + (\sigma_{d/\omega=0} + A\omega^m) D^{-\frac{1}{2}} l^{\frac{1}{2}} + B e_i^{(n_0 - n_1 e_i)}. \quad (27)$$

The parameters  $\alpha$  and  $q$  appearing in Eq. (21) can be determined by three control points of the experimental temperature curve  $\sigma_s(T)$ : 0 ( $\sigma_{s0}, T_0$ ), 1 ( $\sigma_{s1}, T_1$ ), and 2 ( $\sigma_{s2}, T_2$ ), shown in Fig. 4.

$$q = \frac{\ln \frac{\ln(\sigma_{s2}/\sigma_{s0})}{\ln(\sigma_{s1}/\sigma_{s0})}}{\ln(\Delta \bar{T}_2/\Delta \bar{T}_1)}, \quad \alpha = -\frac{\ln(\sigma_{s1}/\sigma_{s0})}{\Delta \bar{T}_1^q} = -\frac{\ln(\sigma_{s2}/\sigma_{s0})}{\Delta \bar{T}_2^q}, \quad (28)$$

where  $\Delta \bar{T} = \Delta T / \Delta T_{\max} = (T - T_0) / (T_{\max} - T_0)$ .

For  $q = 1$  the relation (21) results in a straight line within the plane  $\ln(\sigma_s/\sigma_s^{(is)})$  vs.  $T$  (cf., Fig. 4). However, experimental research on the temperature dependence for mechanical characteristics of some constructional carbon and alloyed steels have shown that physico-structural changes, in particular, temperature allotropy related to lattice rearrangement, result in a non-linear relation  $\ln(\sigma_s/\sigma_s^{(is)})(T)$ . In this case, the parameter  $q$ , which allows for polymorphic transformations in processed material, is greater than 1.

It is convenient to express Eq. (21) as follows

$$\sigma_s = \sigma_s^{(is)} \exp(-\alpha \Delta \bar{T}^q), \quad (29)$$

The rheological dependence (21) quite satisfactorily describes the change of the yield stress during plastic deformation for many structural metals used in mechanical and aeronautic engineering. The temperature dependence of the yield stress is deduced from the fundamental equations of thermodynamics for deformed metals [41]. Clearly, new engineering metallic materials are constantly being developed, and a study of their rheological behavior under plastic deformation will require a generalization of the dependence (21) or even use of essentially new models. This remark is also relevant for the experimentally established Eq. (26) for the stress required for the movement of locked dislocations.

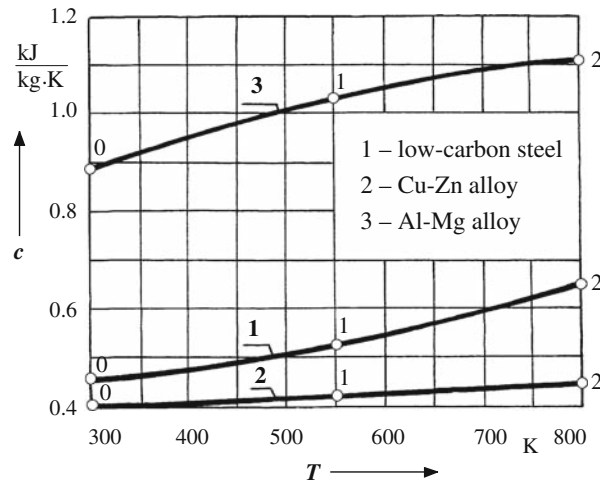


**Fig. 5** Temperature dependence for the specific heat,  $c(T)$

The increase in temperature of the material due to the dissipation of forming energy can be determined from the following energy relation:

$$dw = c\rho dT + du^{(\mu)}, \quad (30)$$

where  $w$  denotes the density of the work of deformation,  $c$  is the specific heat and  $u^{(\mu)}$  is an internal dissipation of the energy related to changes in the structural parameters  $\mu_k$ . According to Eq. (30) not all of the work associated with plastic deformation is converted into heat. Part of it is spent on the change of the structure of the material. Thus, the density of the internal energy ( $u_h$ ) required for hardening is taken as a measure of internal dissipation of the energy, i.e.,  $u^{(\mu)} = u_h$ . Its increment is related to an increment of the density of the deformation work, according to  $du_h = k^{(u_h)}dw$  with a conversion factor  $k^{(u_h)} = 0.1\text{--}0.15$ . The factor  $k^{(u_h)}$  was experimentally determined by [2] as the difference between supplied work of deformation and heat energy generated due to plastic dissipation. The heat energy was quantified by calorimetric tests. As a result, Eq. (30) becomes:

$$(1 - k^{(u_h)}) dw = c\rho dT, \quad (31)$$

By setting  $dw_i = \sigma_i de_i = \sigma_s de_i$  we obtain:

$$dT = \frac{(1 - k^{(u_h)}) \sigma_i}{c\rho} de_i. \quad (32)$$

The temperature dependence for the specific heat (cf., Fig. 5) can be approximated as follows

$$c = c_0 \exp(\beta \Delta \bar{T}^s), \quad (33)$$

where  $c_0$  is the specific heat at the initial temperature  $T_0$  and  $\beta, s$  are parameters which have been found by three points 0 ( $c_0, T_0$ ), 1 ( $c_1, T_1$ ), and 2 ( $c_2, T_2$ ) of the experimental curve for the specific heat shown in Fig. 5:

$$s = \frac{\ln \frac{\ln(c_2/c_0)}{\ln(c_1/c_0)}}{\ln(\Delta \bar{T}_2/\Delta \bar{T}_1)}, \quad \beta = \frac{\ln(c_1/c_0)}{\Delta \bar{T}_1^s} = \frac{\ln(c_2/c_0)}{\Delta \bar{T}_2^s}. \quad (34)$$

For calculations it is convenient to choose control points with the coordinates  $\Delta \bar{T}_0 = 0, \Delta \bar{T}_1 = 0, 5, \Delta \bar{T}_2 = 1$  that are sufficiently distant from each other.

The parameters required for the construction of non-isothermal hardening curves are presented in Table 2 for some plastically deformable materials.

The values of these parameters can vary over some interval due to scattering of the structural and mechanical properties of deformed metals under as-delivered conditions. The applied experimental methods (e.g., X-ray

**Table 2** Material parameters of some plastically deformable materials

Material	Dislocation content, $\rho^*$ , $\text{cm}^{-2}$	Scalar measure of initial damage, $\omega_0$	Measure of locking, $k_y$ , $\text{MPa} \times \text{mm}^{-1/2}$	Average diameter of grain, $D$ , mm	Initial yield strength, $\sigma_{0,2}$ , MPa	Parameters of strain hardening		Parameters of dependence $\sigma_s(T)$		Parameters of dependence $c(T)$			
						$B$ , MPa	$n_0$	$n_1$	$\alpha$	$q$	$c_0$ , $\frac{\text{kJ}}{\text{kg}\cdot\text{K}}$	$\beta$	$s$
Low-carbon steel	$10^9 - 10^{10}$	0.15 – 0.25	12.50	0.016	250	391	0.435	0.097	0.177	2.691	0.450	0.367	1.291
Cu-Zn alloy	$10^{10} - 10^{11}$	0.15 – 0.25	7.77	0.040	176	461	0.600	0.212	0.431	1.823	0.400	0.118	1.076
Al-Mg alloy	$10^{10} - 10^{11}$	0.15 – 0.25	18.54	0.040	237	273	0.439	0.267	1.380	1.000	0.886	0.223	0.572

diffraction, electron microscopy, dilatometry, differentially-thermal method, etc.) have a very high accuracy of measurement of material constants. However, a combined use of all these methods during the determination of the material constants in constitutive equations for the stresses and strains might influence the accuracy in a negative manner. How much this is exactly could be determined inversely by applying these constitutive equations to complex forming experiments numerically and – under the assumption that, in principle, these equations describe the material properly – by comparison of the simulations to actual experiments.

In view of  $\sigma_i = \sigma_s$  and substituting  $\sigma_s$  and  $c$  from Eqs. (29), (33) to Eq. (32) we have:

$$dT = \frac{(1 - k^{(u_h)}) \sigma_i^{(is)} \exp(-\alpha \Delta \bar{T}^q)}{c_0 \rho \exp(\beta \Delta \bar{T}^s)} de_i. \tag{35}$$

Since  $\sigma_i^{(is)} de_i = dw_i^{(is)}$  and  $\Delta T = \Delta T_{\max} \Delta \bar{T}$  it follows after separation of variables and integration that:

$$\int_0^{\Delta \bar{T}} \exp(\alpha \Delta \bar{T}^q + \beta \Delta \bar{T}^s) d(\Delta \bar{T}) = \frac{(1 - k^{(u_h)}) w_i^{(is)}}{c_0 \rho \Delta T_{\max}}. \tag{36}$$

The auxiliary functions  $U(\Delta \bar{T}) = \int_0^{\Delta \bar{T}} \exp(\alpha \Delta \bar{T}^q + \beta \Delta \bar{T}^s) d(\Delta \bar{T})$  and  $U(e_i) = \frac{(1 - k^{(u_h)}) w_i^{(is)}}{c_0 \rho \Delta T_{\max}}$  (cf., Fig. 6) allow to determine a relation between the deformed specimen temperature increment  $\Delta T$  and the strain  $e_i$  (cf., Fig. 7), i.e., the dependence  $T(e_i, \dot{e}_{i0}, T_0, \mu_{k0})$  in Eq. (21), and then to construct non-isothermal hardening curves (cf., Fig. 8).

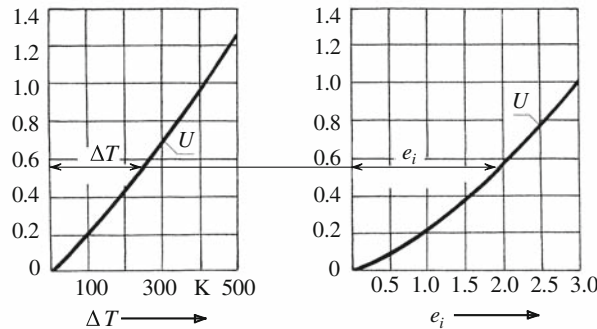


**Fig. 6** Graphic representation of the function  $\Delta T = \Delta T(e_i)$  by means of the auxiliary functions  $U(\Delta T)$  and  $U(e_i)$  for the deformation of low-carbon steel

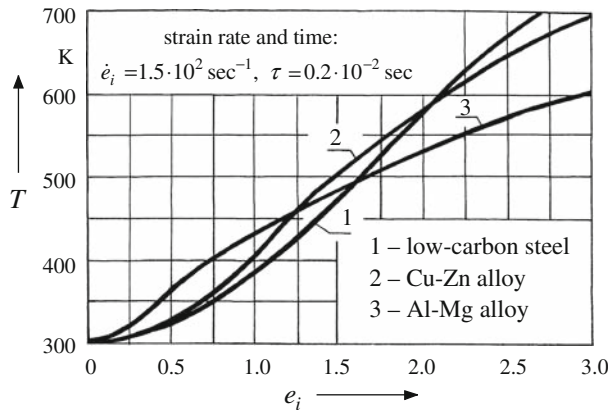


**Fig. 7** Relation between the specimen temperature  $T$  and the strain  $e_i$

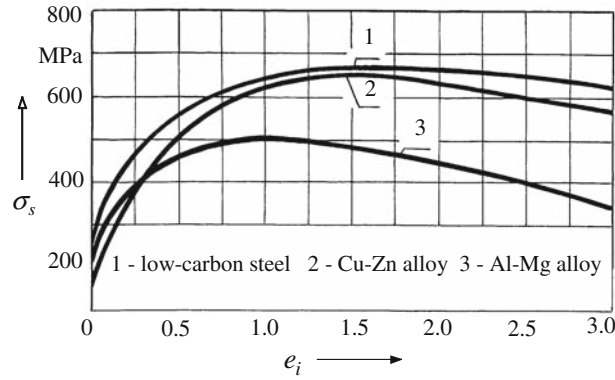


Fig. 8 Non-isothermal hardening

Consequently, in view of Eqn (21), the yield condition shown in Eq. (11) can be rewritten as follows:

$$\frac{1}{2} s_{:j}^i s_{:i}^j - \left( \tau_s^{(is)} \right)^2 \exp \left[ -2\alpha \left( \frac{T - T_0}{T_{\max} - T_0} \right)^q \right] = 0. \quad (37)$$

By putting  $s^2 = (1/2) s_{:j}^i s_{:i}^j$  the differential of the yield function can be expressed as (see Eq. (15)):

$$\begin{aligned} d'f = & 2s \frac{\partial s}{\partial s^{ij}} s^{ij} - 2\tau_s^{(is)} \exp \left[ -2\alpha \left( \frac{T - T_0}{T_{\max} - T_0} \right)^q \right] \\ & \times \left[ -\alpha q \tau_s^{(is)} \left( \frac{T - T_0}{T_{\max} - T_0} \right)^{q-1} d \left( \frac{T - \Delta T_s}{T_{\max} - T_0} \right) + \frac{\partial \tau_s^{(is)}}{\partial \mu_k} d' \mu_k \right]. \end{aligned} \quad (38)$$

The scalar  $h$  takes on the following form (see Eq. (19)):

$$\begin{aligned} h = & \frac{1}{4 \tau_s^{(is)} s} \exp \left[ 2\alpha \left( \frac{T - T_0}{T_{\max} - T_0} \right)^q \right] \times \left( \frac{\partial s}{\partial s^{ij}} \right)^{-1} \\ & \times \left[ \frac{\partial \tau_s^{(is)}}{\partial e_{ij}} - K_s \alpha q \tau_s^{(is)} \frac{(T - T_0)^{q-1}}{(T_{\max} - T_0)^q} + A_s \frac{\partial \tau_s^{(is)}}{\partial \chi_s} + B_s \frac{\partial \tau_s^{(is)}}{\partial \mu_k} \right]^{-1}. \end{aligned} \quad (39)$$

Thus, the scalar multiplier  $d\lambda$  (see Eq. (13)) which connects the strain increments  $de_{ij}$  with a “movement” of the load surface  $f$  is known.

Experimental research of the deformation of steel shows that the thermal flux leads to a noticeable temperature increase of 300–400 K and to a reduction of the yield strength for large finite strains by 100–150 MPa. The density of the work of deformation decreases accordingly when compared with isothermal conditions of the process. The error of calculation for the processing force and the tool pressure can reach 20–30 % if the thermal flux effect is not taken into account.

#### 4 Kinetic equations for structural parameters

The exact form of the kinetic Eq. (5) can be determined on the basis of experimental studies on deformed materials under various processing conditions. The analysis of metallic components which operate at intense loads shows that damage induced by micro-defects, polycrystalline unit grain size, and the internal energy of hardening are the structural properties that greatly influence their service performance. We summarize them as meso-structural parameters.

#### 4.1 Constitutive equations of a tensor theory for strain damage induced by micro-defects

A development of the dislocation arrangement and follow-up dissipative propagation of submicroscopic voids and submicroscopic cracks occur at the initial stage of deformation. Micro-void generation, growth, coalescence, and, finally, macro-crack formation (meaning macro-fracture) are observed during further increasing deformation. The formation of voids is of great importance for the evolution of the strain damage in ductile metals (cf., e.g., [39,40]).

The experimental work of several researchers allows us to determine a range of the damage values related to a nucleation of cavernous defects and discontinuities as a result of the intense coalescence of separate voids (cf., e.g., [3,9,25,34]). Cavernous defects appreciably affect the operating characteristics of finished products. Reaching the critical damage range by the material subjected to working or processing loads can be considered as a micro-fracture criterion.

Two mechanisms of void generation and growth are possible under plastic deformation of metals:

- due to a vacancy flux under the influence of tensile stresses at grain boundaries;
- due to nuclei of voids and discontinuities at triple junctions of grains and nearby large grain-boundary angles under the action of local stress concentration during grain-boundary slip.

Void formation is promoted by diffusion processes as well as by a low mobility of meso-structural elements (such as sub-grains, particles of inclusions, etc.) where voids arise. As a concept of damage a scalar quantity  $\omega$  is traditionally used in solid mechanics in order to describe the accumulation of defects during deformation (Kachanov, 1986):

$$\frac{d\omega}{dt} = \dot{\omega}(\lambda_k^{(\omega)}), \quad i = 1, 2, \dots, \quad (40)$$

where  $\dot{\omega}(\lambda_k^{(\omega)})$  is a damage rate function of parameters  $\lambda_k^{(\omega)}$  which are related to a stress state of the forming process. The damage value varies within the range  $\omega \in [0; 1]$  where  $\omega = 0$  corresponds to the initial state of the material (the undamaged structure) and  $\omega = 1$  corresponds to the moment of macro-destruction. The strain damage results in plastic dilatation of the structure of the metal. The residual relative increase in volume (i.e., the linear invariant  $\varepsilon_{.i}^i$  of the tensor of plastic strains  $\varepsilon_{ij}$ ) is taken as a measure of plastic dilatation. A critical value  $\varepsilon_{.i\text{cr}}^i$  of plastic dilatation is used to characterize the onset of macro-crack formation.

The connection between plastic dilatation and the dissipative formation and growth of strain meso-defects allows to use the linear invariant  $\varepsilon_{.i}^i$  for the parameter  $\lambda_k^{(\omega)}$  in Eq. (40), i.e., we put  $\lambda_k^{(\omega)} = \varepsilon_{.i}^i$ . Thus, the kinetic equation (40) can be expressed as:

$$\frac{d\omega}{dt} = \frac{\dot{\varepsilon}_{.i}^i}{\varepsilon_{.i\text{cr}}^i}, \quad (41)$$

where  $\dot{\varepsilon}_{.i}^i$  denotes a rate of plastic dilatation.

The known models of void growth [14,27,31] consider the volume fraction of voids as a measure of damage:

$$f_v = \frac{\Delta V_v}{\Delta V_{RVE}}, \quad (42)$$

where  $\Delta V_v$  denotes the volume occupied by voids within the representative volume element  $\Delta V_{RVE}$ . The corresponding kinetic equation for damage is written as follows:

$$\frac{df_v}{dt} = (1 - f_v) \dot{\varepsilon}_{.i}^i, \quad (43)$$

Equation (43) characterizes a change in damage due to dilatation of the material resulting from void growth (just as the kinetic Eq. (41) does for  $\omega$ ). The differential relation between the measures  $f_v$  and  $\omega$  follows from Eqs. (41) and (43):

$$\frac{1}{1 - f_v} \frac{df_v}{dt} = \dot{\varepsilon}_{.i\text{cr}}^i \frac{d\omega}{dt}. \quad (44)$$

**Table 3** Chemical composition of studied steels

Steel	Chemical elements, percents by mass					
	Fe	C	W	Mo	V	Cr
Hot-rolled steel	Base	0.88	6.05	5.25	1.95	4.01
Powdered steel	Base	0.97	6.05	5.18	1.91	4.07

While the important role of plastic dilatation as a factor in the assessment of damage for plastically deformed metals is unquestioned [26], it is also necessary to note an influence of the shape of the defects and their direction on the evolution of the strain damage [16,20,24]. Voids assume an elongated ellipsoidal shape under large plastic deformation. At the same time, it turns out that a spatial orientation of the principal axes of the meso-ellipsoids is related to the directions of the principal strains  $\varepsilon_1, \varepsilon_2, \varepsilon_3$  of material particles containing a void. Thus, metals possess tensor properties of strain damage [5,28]. In order to estimate the damage of deformed materials, which is related to volume, shape, and direction of defects, we introduce a symmetric second-rank order tensor  $\omega_{ij}$  by the following differential equation:

$$\frac{d\omega_{ij}}{dt} = \dot{\omega}_{ij}(\lambda_k^{(\omega)}), \quad k = 1, 2, \dots, \quad (45)$$

where  $\dot{\omega}_{ij}(\lambda_k^{(\omega)})$  denotes the dependence of the strain damage tensor on the parameters related to the stress state of the processes.

Decomposition of the tensor of damage increments  $d\omega_{ij} = \dot{\omega}_{ij} dt$  into the hydrostatic tensor  $d\omega_{ii}$  and the deviator  $d\hat{\omega}_{ij}$  makes clear physical sense: the hydrostatic tensor  $d\omega_{ii}$  describes the damage increment caused by a change in volume, and the deviator  $d\hat{\omega}_{ij}$  accounts for the damage increment related to a change of defect shape. Such a view on damage kinetics enables us to apply two integral measures for damage assessment, namely:

$$\begin{aligned} \omega_1 &= \int_{\lambda_k^{(\omega)}(t)} I_1 [\dot{\omega}_{ij}(\lambda_k^{(\omega)})] dt = \int_{\lambda_k^{(\omega)}(t)} \dot{\omega}_{i,i}^j(\lambda_k^{(\omega)}) dt, \\ \hat{\omega}_2 &= 2 \int_{\lambda_k^{(\omega)}(t)} \sqrt{I_2 [\hat{\omega}_{ij}(\lambda_k^{(\omega)})]} dt = \int_{\lambda_k^{(\omega)}(t)} \sqrt{2\dot{\omega}_{i,j}^i \dot{\omega}_{i,i}^j} dt \equiv \int_{\lambda_k^{(\omega)}(t)} \sqrt{2(\dot{\omega}_{i,j}^i \dot{\omega}_{i,i}^j - \dot{\omega}_{i,i}^i \dot{\omega}_{i,j}^j)} dt, \end{aligned} \quad (46)$$

where  $I_1(\dot{\omega}_{ij})$  and  $I_2(\hat{\omega}_{ij})$  are the first invariant of the damage rate tensor  $\dot{\omega}_{ij}$  and the second invariant of the damage rate deviator  $\hat{\omega}_{ij}$ , respectively. In physical terms the measure  $\omega_1$  in Eq. (46) is identically equal to the same measure  $\omega$  in dissipative damage theory (Eqs. (40), (41)). This correspondence allows us to determine  $\omega_1$  by solving Eq. (41).

In view of the relationship  $\varepsilon_i^i(\Lambda)$  between the plastic dilatation and the cumulative strain (cf., Eq. (12)) Eq. (41) becomes:

$$\frac{d\omega_1}{dt} = \frac{1}{\varepsilon_i^i(\Lambda_{\text{lim}})} \cdot \frac{d\varepsilon_i^i(\Lambda)}{d\Lambda} \cdot \frac{d\Lambda}{dt} \equiv \frac{[\varepsilon_i^i(\Lambda)]' \dot{\Lambda}}{\varepsilon_i^i(\Lambda_{\text{lim}})}. \quad (47)$$

where  $\Lambda_{\text{lim}}$  denotes a limit value of shear strain corresponding to the point of destruction, and the dash refers to differentiation with respect to  $\Lambda$ .

The function  $\varepsilon_i^i(\Lambda)$  can be determined on the basis of a pycnometric analysis of change of the initial density of deformed materials. Plastic dilatation was studied for multi-component alloyed steels made by two manufacturing techniques: hot rolling and powder metallurgy (cf., Table 3). These steels are of essentially different grain structures. The powdered steel has finer ferrite grains and evenly distributed small carbides in contrast to the hot-rolled steel (cf., Table 4). The values of the structural parameters were obtained by radiographic analysis. The selection of two materials with identical chemical compositions and essentially different micro-structures allows us to study an effect of their micro-structural properties on the evolution of strain damage. The test specimens were subjected to uniaxial tension up to their macro-destruction (fracture).

**Table 4** Structural parameters of studied steels

Steel	$\rho^*$ , $\text{cm}^{-2}$	Ferrite lattice parameter, nm	Ferrite grain size, $\mu\text{m}$	Carbide size, $\mu\text{m}$	Distance between carbides, $\mu\text{m}$	Phase, percents by volume		
						Carbide $\text{M}_6\text{C}$	Carbide $\text{MC}$	Ferrite
Hot-rolled steel	$5 \times 10^{11}$	0.2872	11.3 – 14.5	2.90 – 3.70	3.3 – 4.1	15	2	83
Powdered steel	$10^9$	0.2871	3.7 – 4.5	0.99 – 1.21	0.73 – 0.87	14	4	82

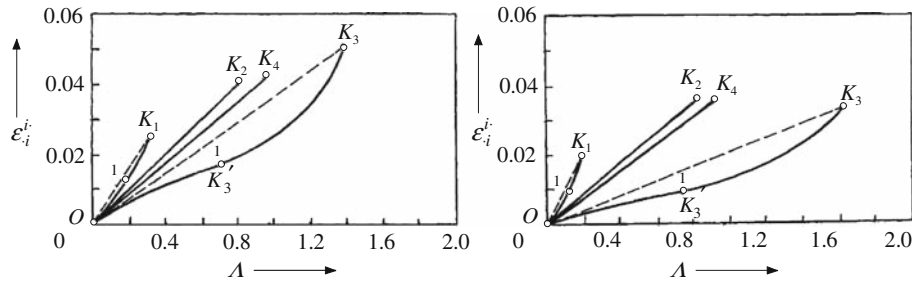


**Fig. 9** Plastic dilatation ( $\varepsilon_i^i$ ) dependence on shear strain ( $\Lambda$ ): *left* hot-rolled steel (C 0,88 %, W 6,05 %, Mo 5,25 %, V 1,95 %, Cr 4,01 %); *right* powdered steel (C 0,97 %, W 6,05 %, Mo 5,18 %, V 1,91 %, Cr 4,07 %);  $K_1$  20°C;  $K_2$  750°C;  $K_3$  830°C;  $K_4$  870°C; *dashed line* linear model of plastic dilatation

**Table 5** Parameters of plastic dilatation of studied steels

Parameters	Hot-rolled steel				Powdered steel			
	20	750	810 – 825	850	20	750	810 – 825	850
Strain temperature °C	20	750	810 – 825	850	20	750	810 – 825	850
$a$	1.170	1.000	$0.339\Lambda + 1.259$	1.000	1.484	1.000	$0.291\Lambda + 1.212$	1.000
$b$	0.092	0.049	0.0279	0.043	0.218	0.043	0.0147	0.038

**Table 6** Temperature of phase transformations (results from the dilatometric analysis)

Material	Point $A_{c1}$ °C	Point $A_{SP}$ °C
Hot-rolled steel	830 – 840	880 – 890
Powdered steel	815 – 825	870 – 880

In Fig. 9 the experimentally determined dependence of plastic dilatation on strain is shown for various temperatures for two multi-component alloyed steels.

The dependencies obtained for the plastic dilatation of steels allow us to draw the following conclusions. The experimental dependence  $\varepsilon_i^i(\Lambda)$  can be approximated by the following power function:

$$\varepsilon_i^i = b\Lambda^a, \tag{48}$$

where  $a$  and  $b$  have been found by control points 1 ( $\varepsilon_{i1}^i, \Lambda_1$ ) and  $K$  ( $\varepsilon_{i,cr}^i, \Lambda_{lim}$ ) of the experimental curve  $\varepsilon_i^i(\Lambda)$  (cf., Table 5):

$$a = \frac{\ln(\varepsilon_{i,cr}^i / \varepsilon_{i1}^i)}{\ln(\Lambda_{lim} / \Lambda_1)}, \quad b = \frac{\varepsilon_{i1}^i}{\Lambda_1^a} = \frac{\varepsilon_{i,cr}^i}{\Lambda_{lim}^a}. \tag{49}$$

The point  $K$  corresponds to the moment of fracture (cf., Fig. 9).

For cold deformation the function of plastic dilatation (48) assumes an exponent  $a > 1$  (Fig. 9, curve  $OK_1$ ). In the case of under-hot and hot forming the experimental diagrams  $OK_2$  and  $OK_4$  are very close to linear approximations. For such conditions a linear dependence with  $a = 1$  is used. Super-plastic (SP) forming of steels was realized in the temperature interval  $[A_{c1}; A_{SP}]$  corresponding to the diffusive phase transformation ( $\alpha \rightarrow \gamma$ ) of the investigated steels (cf., Table 6). Therefore, a more complex function with a

variable exponent  $a = a(\Lambda)$  is required for super-plastic deformation (Fig. 9, curve  $OK_3$ ):

$$\varepsilon_i^i = b\Lambda^{a(\Lambda)} = b\Lambda^{(l_1\Lambda + l_0)}. \quad (50)$$

The condition  $d^2\varepsilon_i^i/d\Lambda^2 = 0$  in the inflection point  $K'_3$  is added to Eq. (49) for calculating  $b$ ,  $l_0$ ,  $l_1$ . Thus, a third dependence between these parameters results:

$$\frac{1}{\Lambda} \left( l_1 - \frac{l_0}{\Lambda} \right) + \left( l_1 \ln \Lambda + l_1 + \frac{l_0}{\Lambda} \right)^2 = 0. \quad (51)$$

The crucial stage of super-plastic deformation is the evolution of the inflection point  $K'_3$ , which separates the areas of delayed ( $OK'_3$ ) and the accelerated ( $K'_3K_3$ ) development of damage in steels.

In view of Eq. (48) the differential equation (47) and integral dependency (46) for  $\omega_1$  now become:

$$\frac{d\omega_1}{dt} = \frac{[b\Lambda^{a(\Lambda)}]'\dot{\Lambda}}{b\Lambda_{lim}^a} \equiv \frac{(\frac{a}{\Lambda} + a' \ln \Lambda) \Lambda^a \dot{\Lambda}}{\Lambda_{lim}^a}, \quad \omega_1 = \int_{\Lambda(t)} \frac{(\frac{a}{\Lambda} + a' \ln \Lambda) \Lambda^a \dot{\Lambda}}{\Lambda_{lim}^a} dt. \quad (52)$$

Micro-fractograms in Fig. 10 have been obtained with the purpose of a more detailed understanding of the fracture type for W-Mo steels at uniaxial tension under superplasticity conditions. The fracture surface contains a dimple-type structure indicating ductile fracture. Meso-elements of the structure are rather elongated and tracks of intragranular or phase-boundary shifts are visible on some of their surfaces. Porosity in fractures is thus obvious. Separate areas with cup and quasi-cleavage fracture are visible in the fractogram of the hot-rolled steel in Fig. 10a, because of its high structural heterogeneity. These regions of fracture indicate an irregularity of superplastic deformation behavior. Such areas are missing in the powdered steel. The results of micro-structural and fractographic studies show that deformation of both the steels under optimum temperature-rate superplastic conditions allows attaining high strains even at uniaxial tension (when predominant tensile stresses promote voids opening). The powdered steel has a ductility resource appreciably greater than the hot-rolled steel owing to the finer granularity of its structure.

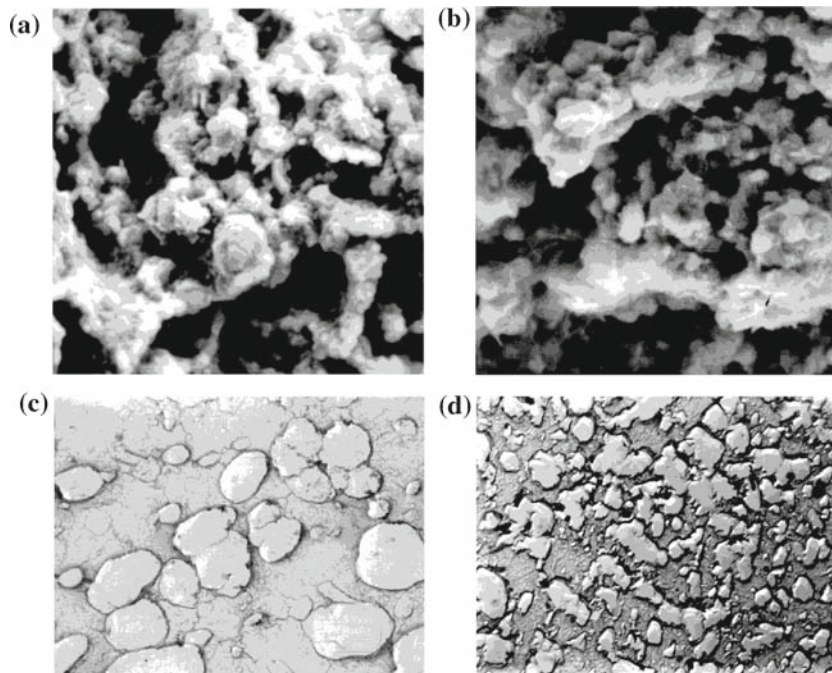


**Fig. 10** Electronic fractograms and replicas of the steels after deformation under conditions of superplasticity. **a** Fractogram of the hot-rolled steel ( $\times 3,000$ ), **b** fractogram of the powdered steel ( $\times 3,000$ ), **c** replica of the hot-rolled steel, damage  $\omega < 0.75-0.80$  ( $\times 5,000$ ) **d** replica of the powdered steel damage  $\omega < 0.75-0.80$  ( $\times 5,000$ )

An electronic-micro-structural analysis of the specimens obtained under stage-by-stage deformation has been carried out to study the evolution of structural damage. The analysis of electronic replicas (Fig. 10c, d) allows to reveal a stage of active voids coalescence. For these steels the intense voids coalescence occurs under deformation corresponding to damage  $\omega_1 > 0.75$ – $0.85$ . The obtained results are very important for a definition of operational strain in the manufacturing processes designed for the products with high working characteristics.

The kinetic equation (47) contains the limit strain  $\Lambda_{\text{lim}}$ . Experimental research by [6] shows that the metal ductility (i.e., the limiting strain) is effected by stress state, temperature-speed conditions of processing, chemistry and the structure of metals, i.e.:

$$\Lambda_{\text{lim}} = \Lambda_{\text{lim}}(\sigma^{ij}, \dot{e}_{ij}, T, \mu_k). \quad (53)$$

The experimental determination of the dependence indicated in Eq. (53) requires a complex system of tests for each material. It is convenient to specify Eq. (53) by means of plasticity diagrams (cf., Fig. 11) which connect the limit strain  $\Lambda_{\text{lim}}$  with characteristics of the stress state.

The basic characteristic is triaxiality, i.e., a combination of invariants  $\bar{\sigma} = \frac{1}{3}I_1(\sigma_{ij})/I_2^{1/2}(s_{ij})$ . The other characteristic is the stress phase  $\phi_\sigma$ , i.e., a combination of invariants  $I_3(s_{ij})/I_2^{3/2}(s_{ij})$ . The presented diagram of plasticity is made for metals with specified chemical composition and structure  $\mu_{k0}$  under fixed temperature-speed conditions of processing, viz.,  $\dot{e}_{ij0}$ ,  $T_0$ . Obviously with increasing triaxiality the limit strain of the material decreases but the damage increases (cf., Eq. (52)<sub>2</sub>), and vice versa.

In physical terms and according to Eq. (46)  $\hat{\omega}_2$  is a damage measure connected with a change of the void shape during the plastic deformation of the metal. As shown by specialized experimental research the void shape elongated in a direction of the principal tensile strain  $\varepsilon_1$  promotes the void growth and coalescence [19,37]. The equivalent increment of the deviatoric strain of voids is taken as a measure of the void shape change during the short time period  $dt$ :

$$d\hat{e} = \dot{\hat{e}} dt = \sqrt{\frac{1}{2} \left( \dot{\hat{e}}_{\cdot j}^i \dot{\hat{e}}_{\cdot i}^j \right)} dt, \quad (54)$$

where  $\dot{\hat{e}}_{\cdot j}^i$  are deviatoric strain rates related to the voids.

The moment of critical value  $\hat{e}_{\text{cr}}$  of equivalent strain of voids relates to a stage of intense coalescence of ellipsoidal voids and to the formation of cavernous defects with sizes up to  $20$ – $30 \mu\text{m}$ . This relation allows us

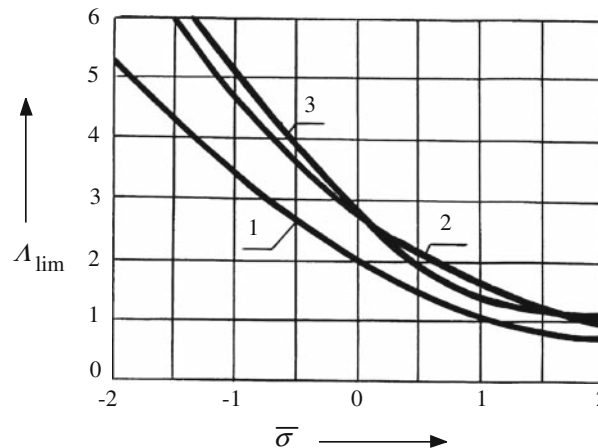


**Fig. 11** Diagrams of plasticity of constructional materials under as-delivered conditions: 1 low-carbon low-alloy steel, 2 Cu-Zn alloy, 3 Al-Mg alloy

to formulate the following kinetic equation:

$$\frac{\varepsilon_{\text{cr}}}{\widehat{\mathbf{e}}_{\text{cr}}} \frac{d\widehat{\omega}_2}{dt} = \frac{d\omega_2}{dt} = \frac{\dot{\widehat{\mathbf{e}}}}{\widehat{\mathbf{e}}_{\text{cr}}}, \quad (55)$$

where  $\omega_2 = \left( \varepsilon_{\text{cr}} / \widehat{\mathbf{e}}_{\text{cr}} \right) \widehat{\omega}_2$ .

The normalizing factor  $\varepsilon_{\text{cr}} / \widehat{\mathbf{e}}_{\text{cr}}$  allows us to introduce the damage measure  $\omega_2 \in [0; 1]$  which is convenient for comparing the calculations. Interval boundaries correspond to the initial (strainless) state of the material and to a stage of intense void coalescence (the micro-fracture stage). The integrated value of the parameter reads:

$$\omega_2 = \int_t \frac{\dot{\widehat{\mathbf{e}}}}{\widehat{\mathbf{e}}_{\text{cr}}} dt \equiv \int_t \frac{\sqrt{(1/2) \left( \dot{\widehat{\mathbf{e}}}_j^i \dot{\widehat{\mathbf{e}}}_i^j \right)}}{\widehat{\mathbf{e}}_{\text{cr}}} dt = \int_t \frac{\varepsilon_{\text{cr}}}{\widehat{\mathbf{e}}_{\text{cr}}} \sqrt{\frac{1}{2} \dot{\widehat{\omega}}_j^i \dot{\widehat{\omega}}_i^j} dt \equiv \int_t \frac{\varepsilon_{\text{cr}}}{\widehat{\mathbf{e}}_{\text{cr}}} \sqrt{\frac{1}{2} \left( \dot{\omega}_j^i \dot{\omega}_i^j - \dot{\omega}_i^i \dot{\omega}_j^j \right)} dt. \quad (56)$$

For calculating the damage parameter  $\omega_2$  during plastic flow of metals it is necessary to construct a geometrical model to describe the change of the shape of the void. Stresses, strains, strain rates and temperatures as well as connected properties of the deformed material studied in continuum mechanics are local parameters, i.e., they relate to small volumes ( $\Delta V$ ). Small volumes  $\Delta V$  of engineering metals (with linear dimensions  $\Delta s = 35\text{--}140 \mu\text{m}$ ) include meso-volumes ( $\Delta V_{\text{meso}}$ ) with meso-structural elements (grains, voids, dislocation cells with linear dimensions  $\Delta s_{\text{meso}} = 3\text{--}18 \mu\text{m}$ ). Thus, the volume ratio is  $\Delta V_{\text{meso}} / \Delta V = (6.3\text{--}21.3) \times 10^{-4}$ .

In a number of publications the physical model of the ductile damaged material (obviously, based on the afore-mentioned volume ratio) corresponds to the volume element ( $\Delta V$ ) with a representative distribution of micro-defects (with the volume  $\Delta V_{\text{meso}}$ ), (cf., Fig. 12). For developing a mathematical model of ductile damaged material the representative volume element  $\Delta V$  (RVE) is often idealized as an elementary rectangular parallelepiped with a regular distribution of micro-defects, i.e., voids [9]. In earlier papers a sphere, and a circular or elliptic cylinder were assumed as elementary void shapes [11, 14, 27, 31]. The ellipsoidal shape of voids with a variable ratio between the principle axes was used in later papers [7, 9, 10, 42]. The ellipsoidal model allows us to describe the damage evolution in deformed materials much more precisely in view of both the void volume growth as well as the change of the void shape. It is also worth mentioning that the ellipsoidal shape allows us to model the void coalescence satisfactorily.

In the present paper the model of an ellipsoidal void is applied in order to study the processes of complex loading of plastically deformed damaged solids. Under complex loading the ratio between the principal strains  $\varepsilon_1, \varepsilon_2, \varepsilon_3$  changes and the principal strain axes rotate over the material fibers (i.e., w.r.t. an accompanying coordinate system). We consider a meso-volume element  $\Delta V_{\text{meso}}$  with one void (cf., Fig. 13). At the initial moment of the deformation the shape of the particle meso-volume is a cube, and the void shape is a sphere (with the volume  $\Delta V_v(0)$ ). The space orientation of the meso-parallelepiped corresponds to an accompanying coordinate system  $\xi^k, k = 1, 2, 3$ , chosen at the initial moment  $t_0$  (cf., Fig. 13, left). The accompanying

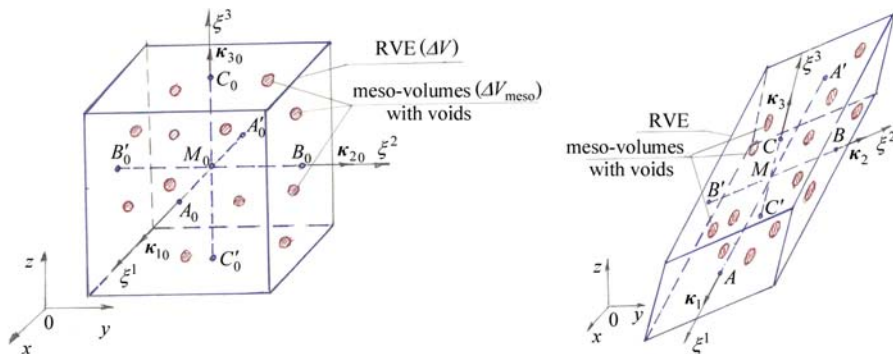


**Fig. 12** Arbitrarily complex deformation of the RVE: *left* initial moment, *right* current moment

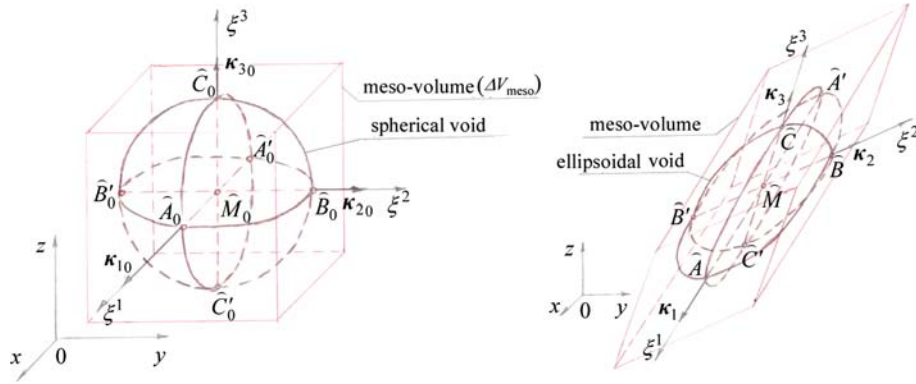


**Fig. 13** Arbitrarily complex deformation of the meso-volume with a single void: *left* initial moment, *right* current moment

axes  $\xi^k$  are rigidly connected with the particles of the continuum and deform concurrently. Therefore, the accompanying Cartesian system of orthogonal coordinates chosen at the initial moment becomes, generally speaking, curvilinear and non-orthogonal under arbitrarily complex deformation. During arbitrarily complex deformation (for the finite period  $\Delta t = t - t_0$ ) the cube-shaped meso-volume transforms into an oblique parallelepiped, and the spherical void transforms into an ellipsoid with the volume  $\Delta V_v$  (cf., Fig. 13, right).

We select in a volume  $\Delta V_{v0}$  of the spherical void three diametric segments ( $\widehat{A_0A'_0}$ ,  $\widehat{B_0B'_0}$ ,  $\widehat{C_0C'_0}$ ) which, at the initial moment  $t_0$ , pass through the center of the sphere,  $\widehat{M_0}$ , in the direction of the coordinates  $\xi^k$ . At the current moment of deformation,  $t$ , they transform into the material segments  $\widehat{AA'}$ ,  $\widehat{BB'}$ ,  $\widehat{CC'}$  of the ellipsoid and the angles between them are  $\widehat{\psi}_{k0} = \pi/2 \Rightarrow \widehat{\psi}_k \neq \pi/2, k = 1, 2, 3$ . These six parameters of the ellipsoid (three linear and three angular) are connected with the metric tensor  $g_{ij}$  of the accompanying axes  $\xi^k$  and allow to determine the void strain  $\widehat{\varepsilon}_{ij}$  with respect to the initial void state as follows [32]:

$$\widehat{\varepsilon}_{ij} = \frac{1}{2} (g_{ij} - g_{ij0}), \quad (57)$$

$$g_{ij} = \kappa_i \cdot \kappa_j = |\kappa_i| \cdot |\kappa_j| \cos \widehat{\psi}_k, \quad g_{ij0} = \kappa_{i0} \cdot \kappa_{j0} = |\kappa_{i0}| \cdot |\kappa_{j0}| \cos \widehat{\psi}_{k0}, \quad (58)$$

where  $\kappa_i, \kappa_{i0}$  are covariant base vectors of the accompanying axes  $\xi^k$  at the current and the initial moment  $t$  and  $t_0$ , respectively;  $\widehat{\psi}_k, \widehat{\psi}_{k0}$  are the angles between the vectors  $\kappa_i$  and  $\kappa_j$  at the current and initial moments.

Covariant components of the void strains can be found as (cf., Appendix):

$$\begin{aligned} \widehat{\varepsilon}_{11} &= \frac{1}{2} \left( \left( \frac{\widehat{AA'}}{\widehat{A_0A'_0}} \right)^2 - 1 \right), \quad \widehat{\varepsilon}_{12} = \frac{1}{2} \frac{\widehat{AA'} \widehat{BB'}}{\widehat{A_0A'_0} \widehat{B_0B'_0}} \cos \left( \widehat{\psi}_3 \right), \\ \widehat{\varepsilon}_{13} &= \frac{1}{2} \frac{\widehat{AA'} \widehat{CC'}}{\widehat{A_0A'_0} \widehat{C_0C'_0}} \cos \left( \widehat{\psi}_2 \right), \dots, \end{aligned} \quad (59)$$

including the mixed components:

$$\begin{aligned} \widehat{\varepsilon}_{\cdot 1}^{\cdot 1} &= \frac{1}{2} \left( 1 - \left( \frac{\widehat{A_0A'_0}}{\widehat{AA'}} \right)^2 \right), \quad \widehat{\varepsilon}_{\cdot 2}^{\cdot 1} = \frac{1}{2} \frac{\widehat{A_0A'_0} \widehat{BB'}}{\widehat{AA'} \widehat{B_0B'_0}} \cos \left( \widehat{\psi}_3 \right), \\ \widehat{\varepsilon}_{\cdot 3}^{\cdot 1} &= \frac{1}{2} \frac{\widehat{A_0A'_0} \widehat{CC'}}{\widehat{AA'} \widehat{C_0C'_0}} \cos \left( \widehat{\psi}_2 \right), \dots, \end{aligned} \quad (60)$$

which are required for the calculation of the volumetric ( $\widehat{\varepsilon}_i^{i\cdot}$ ) and the deviatoric ( $\widehat{\mathbf{e}}$ ) strain of the voids. The principal strains  $\widehat{\varepsilon}_1, \widehat{\varepsilon}_2, \widehat{\varepsilon}_3$  can be found by solving the characteristic equation for the strain tensor:

$$\begin{aligned}\widehat{\varepsilon}_1 &= \frac{1}{3}\widehat{\varepsilon}_i^{i\cdot} + \frac{2}{\sqrt{3}}\widehat{\mathbf{e}} \cos\left(\phi_e - \frac{\pi}{3}\right), & \widehat{\varepsilon}_2 &= \frac{1}{3}\widehat{\varepsilon}_i^{i\cdot} + \frac{2}{\sqrt{3}}\widehat{\mathbf{e}} \cos\left(\phi_e + \frac{\pi}{3}\right), \\ \widehat{\varepsilon}_3 &= \frac{1}{3}\widehat{\varepsilon}_i^{i\cdot} + \frac{2}{\sqrt{3}}\widehat{\mathbf{e}} \cos\phi_e,\end{aligned}\quad (61)$$

where  $\phi_e$  is the Lode angle for the strains.

An experimental determination of the changing sizes of voids is connected with great technical difficulties [23]. This is why we will make use of statistical characteristics of void formation. For instance, the averaged characteristics of the void strain for the present elementary volume  $\Delta V$  can be applied within each RVE. A corresponding measure is the strain ( $\varepsilon_{ij}$ ) of RVE. If at the initial moment  $t_0$  we select in the volume element three material segments ( $A_0A'_0, B_0B'_0, C_0C'_0$ ) which pass through the center  $M_0$  in the direction of the coordinates  $\xi^k$  then they will transform into material segments  $AA', BB', CC'$  at the current moment  $t$ , and the angles between them will be  $\psi_{k_0} = \pi/2 \Rightarrow \psi_k \neq \pi/2, k = 1, 2, 3$ . These six parameters of the RVE allow us to determine its strains  $\varepsilon_{ij}$  by relations analogous to those for the void strain. The hypothesis that it is possible to model the void deformation by using the strain measures of the material volume element requires a detailed experimental verification. The experimental justification of this hypothesis will allow us to predict shape changes and coalescence of voids by means of accompanying axes plotted as coordinate grids on deformed specimens and manufacturing half-stuff.

The determination of the critical equivalent strain  $\widehat{\varepsilon}_{cr}$  of voids in the investigated materials is based on electron-probe analysis of the void coalescence in test specimens during their stage-by-stage plastic deformation. Obtained electronic replicas allow us to detect a stage of intense void coalescence into large cavernous defects (discontinuity flaws). The combined use of two damage measures,  $\omega_1$  and  $\omega_2$ , (in contrast to using only  $\omega_1$  as in previous publications) allows us to predict not only a risk of macro-fracture of the deformed material but also a stage of formation of large cavernous defects due to coalescence of voids taking a change in their shape and orientation into account. This approach is necessary when producing metalware to be operated under intense load and thermal action, high pressure and strain rate. It can be explained by the indisputable fact that a high-quality micro-structure of the metal (without large cavernous defects and clusters) essentially improves an ability of metallic components to withstand dynamic impact loads and also enhances their fatigue resistance. Such products and components are widely used in aerospace, automotive and energy engineering.

#### 4.2 Grain size and internal hardening energy

An essential structural parameter of the deformed metal is the grain size (diameter  $D$ ). The experimental data by [2] show that strain  $\Lambda$ , temperature  $T$  and strain rate  $\dot{\Lambda}$  effect the grain size of processed metals, i.e.:

$$\frac{dD}{dt} = \dot{D}(\Lambda, H, T, \mu_k). \quad (62)$$

Three-dimensional diagrams representing the grain size dependent on strain and temperature (recrystallization diagrams) can be obtained by integrating Eq. (62) for the materials with a specified initial micro-structure  $\mu_{k_0}$  and strain rate  $\dot{\Lambda}_0$ :

$$D(\Lambda, T, \dot{\Lambda}_0, \mu_{k_0}) = \int_0^\Lambda \int_{T_0}^T \dot{D}'(\Lambda, T, \dot{\Lambda}_0, \mu_{k_0}) d\Lambda dT. \quad (63)$$

These integrals represent a set of hypersurfaces in the phase space  $D, \Lambda, \dot{\Lambda}, T, \mu_k$ . For calculations it is convenient to use a set of plane curves  $D = D(\Lambda, T_0, \dot{\Lambda}_0, \mu_{k_0})$  for describing the surface  $D = D(\Lambda, T, \dot{\Lambda}_0, \mu_{k_0})$ . Experimental studies in die forging of low-carbon low-alloy steels allow us to formulate the following form of Eq. (62):

$$\frac{dD}{dt} = -\gamma(\Lambda - \Lambda_0)^{p-1} \dot{\Lambda} D_0 \exp[-\gamma(\Lambda - \Lambda_0)^p], \quad (64)$$

where  $D_0$  is the grain size corresponding to the initial shear strain  $\Lambda_0$ ;  $\gamma(T)$ ,  $p(T)$  are parameters determined by experimental control points.

Recrystallization by annealing recovers ductile properties of processed half-finished products. Thus it is reasonable to predict the grain size by means of recrystallization curves  $D = D(\Lambda_0, T, \dot{\Lambda}_0, \mu_{k0})$  as shown in Fig. 14 (left). Recrystallization curves are used for metal forming with further annealing at the specified temperature. In this case the grain size is determined by the strain  $\Lambda$  and the temperature  $T$  prior to annealing. The kinetic equation of recrystallization is [36]:

$$\frac{dD}{dt} = D_1 \frac{n}{\tilde{t}} \left(1 + \frac{t}{\tilde{t}}\right)^{n-1}, \quad (65)$$

where  $D_1$  is an average diameter of the grain before annealing;  $n$  is the parameter related to temperature;  $\tilde{t}$  denotes a characteristic time of isothermal heating (when the grain size increases  $(2^n - 1)$  times).

In case of isothermal heating the parameter  $n$  does not depend on time. The grain size is determined using the following power dependence:

$$D = D_1 \left[ \left(1 + \frac{t}{\tilde{t}}\right)^n - 1 \right]. \quad (66)$$

The internal energy of hardening  $E_h$  or its density  $u_h = dE_h/d\Omega$  is one of the main factors defining an irreversible change of the crystalline structure of the deformed metal ( $\Omega$  being a volume of the deformed region). According to experimental data obtained by the electron microscopy the internal energy of hardening is close to the total energy of dislocations and connected with a change in the dislocation arrangement as follows. Initially, at small deformation almost all absorbed energy is consumed for creation of the crystalline structure (dislocations) and resistant defects at the current temperature. Defects will still nucleate while the deformation increases. However, some of them vanish as the growing density of the deformation work reduces the activation energy of the defect annihilation due to both a dissipative rise in the temperature and an intensification of the dislocation interaction [2]. This change of the internal energy of hardening is described by the following kinetic equation (cf., Fig. 14, right):

$$\frac{du_h}{dt} = \mu^{(u_h)} \sqrt{I_2(D_\sigma)} \dot{\Lambda}, \quad (67)$$

where  $\mu^{(u_h)}$  denotes the parameter related to strain.

For a number of engineering materials we may write:

$$\mu^{(u_h)} = \mu_0^{(u_h)} \exp(-\Lambda/\Lambda_{lim}), \quad (68)$$

$\mu_0^{(u_h)}$  being an initial value of the parameter  $\mu^{(u_h)}$  (obtained by the experiments).

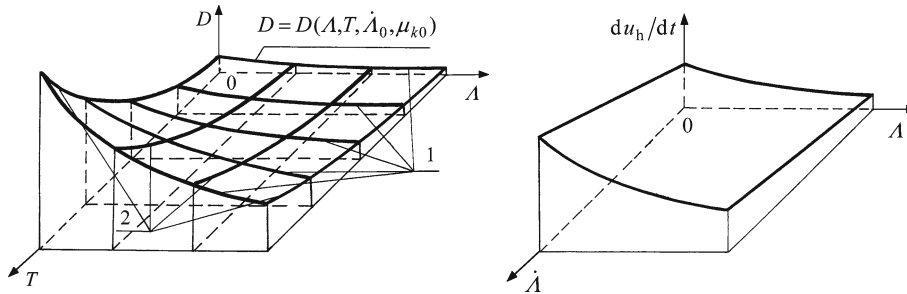


**Fig. 14** Left the integral surface of the kinetic equation (68) in the phase subspace  $D, \Lambda, T$ : 1 supporting curves  $D = D(\Lambda, T_0, \dot{\Lambda}_0, \mu_{k0})$ , 2 supporting curves  $D = D(\Lambda_0, T, \dot{\Lambda}_0, \mu_{k0})$ , right the internal energy of hardening dependent on strain rate  $\dot{\Lambda}$  and shear strain  $\Lambda$

## 5 Conclusions and outlook

Plastic flow theory and continuum damage mechanics provide a theoretical and methodological framework for research and modeling of forming processes for metalware with optimum service properties. Such a combined basis allows us to solve the following problems:

- to formulate a system of constitutive equations for modeling and analyzing metal forming processes together with the prediction of meso-structural properties of deformed materials;
- to create associated physico-mechanical models for the strained material which will describe not only its mechanical behavior but also essential physics properties at a meso-structural level (strain damage, polycrystal unit grain size, internal energy of hardening).

The developed system of basic governing Eqs. (1)–(12) describes large plastic deformations under complex loading conditions typical for a number of metal forming processes (e.g., deep-drawing, die forging, extrusion, super-plastic forming). The possibility of the analysis of non-stationary plastic flow in such forming processes is very important. This necessitates the stage-by-stage determination of the stress-strain state and related meso-structural parameters.

The von Mises yield function includes the yield stress depending on strain, strain rate, temperature, and parameters of the meso-structure. Representation of the yield stress dependence (20) by the hypersurface  $f = 0$  in the phase space  $\sigma_s, e_i, \dot{e}_i, T, \mu_k$  allows its specification for each material by means of non-isothermal hardening curves obtained by tests for different deformation conditions. Based on the systematized experimental data the power dependence (21) of the yield stress on the temperature is proposed. It also arises from the fundamental principles of thermodynamics for deformed metals. The plotting technique for non-isothermal curves is presented for materials with a variable meso-structure when a change in temperature,  $T$ , is connected with a thermal flux effect during the deformation depending on the strain path,  $s$ .

Meso-structural damage parameters of deformed materials appreciably affect the operating characteristics of finished products. A tensor theory of strain damage induced by micro-defects is of great importance from the point of view of a combined physico-mechanical approach. The method offered for determining the symmetric second-rank order tensor of damage makes physical sense as this tensor is decomposed into hydrostatic and deviatoric parts: The hydrostatic tensor describes the evolution of damage connected with a change in volume, while the deviator describes the evolution of damage connected with a change in defect shape. Such a representation of damage kinetics allows to use two integral measures,  $\omega_1$  and  $\omega_2$ . These measures are very important for the estimation of the meso-structure quality of metalware produced by metal forming techniques and subjected to intense power and thermal loads, high strain rates, physico-chemical actions.

A successful practical application of the tensor theory requires rather laborious experimental research on damage kinetics for deformed materials under complex loading. The most urgent problem is the experimental characterization of the material constants appearing in the constitutive equations for damage. Critical plastic dilatation,  $\varepsilon_i^i$ , limiting cumulative strain,  $\Delta_{\text{lim}}$ , critical equivalent strain of void,  $\hat{e}_{\text{cr}}$  are necessary to be considered among these material constants.

Results of the calculations of material constants and parameters relevant to the defining relations were given only for selected materials. Performing similar calculations for other materials will require further complex experiments at the meso-level. Indeed, such experiments will allow us to create a well-founded database for meso-structural properties of plastically deformed materials which is a prerequisite for computer simulations. The presented basic relations and rheological dependencies describe large plastic deformation of many structural metals used in mechanical and aeronautic engineering quite satisfactorily. Naturally, new structural metallic materials are constantly developed and, thus, studies of their rheological behavior under plastic deformation will eventually necessitate a generalization of certain dependencies (e.g., Eqs. (21), (26)) or even require use of fundamentally new models.

It should also be noted that the basic equations of meso-structural damage include stress-strain state characteristics. Therefore, a reliable prediction of damage parameters necessitates an exact determination of the stress fields,  $\sigma^{ij}$ , and of the flow velocity fields,  $v^i$ , in deformed materials allowing for complex loading conditions and the strain path,  $s$ .

In a single paper it is obviously impossible to discuss (even in a compressed form) all the questions pertinent to the presented constitutive equations. In particular this holds for the technically relevant but complicated questions of instabilities in plastically deformed blanks and half-stuffs. The complex problem of stability, which is typical for some processes of sheet metal forming (e.g., deep-drawing, swaging), will be the subject of separate publications. The ultimate goal of the authors is to implement the damage criterion which combines

$\omega_1$  and  $\omega_2$  in numerical solution schemes for metal forming. To this end computational techniques will be developed which, eventually, can be coupled with finite element codes.

**Acknowledgments** The present work was supported by Deutsche Forschungsgemeinschaft (DFG) through the special program for funding research stays in Germany of researchers from Central and Eastern Europe/CIS. This work was also supported by the President Grant for Young Russian Scientists and Their Advisers MK-4126.2006.8, and the Grant of the Albany-Tula Alliance, Inc. (a Restricted Gift from Prof. Charlotte S. Buchanan).

## Appendix

Covariant components for the strain of voids

The covariant base vectors  $\boldsymbol{\kappa}_i$ ,  $\boldsymbol{\kappa}_{i_0}$  change from one point of the deformed solid to another and can be determined by differential dependences:

$$\boldsymbol{\kappa}_i = \frac{\partial \mathbf{r}}{\partial x^i}, \quad \boldsymbol{\kappa}_{i_0} = \frac{\partial \mathbf{r}_0}{\partial x^i}, \quad (\text{A.1})$$

where  $\mathbf{r}$ ,  $\mathbf{r}_0$  denote radius-vectors of points of the deformed solid at the current and initial moments. Moreover we note the following relations for the basis vectors:

$$\frac{|\boldsymbol{\kappa}_i|}{|\boldsymbol{\kappa}_{i_0}|} = \frac{\left| \frac{\partial \mathbf{r}}{\partial \xi^i} \right|}{\left| \frac{\partial \mathbf{r}_0}{\partial \xi^i} \right|} = \frac{|\mathbf{dr}_i|}{|\mathbf{dr}_{i_0}|} = \frac{ds_i}{ds_{i_0}}, \quad (\text{A.2})$$

where  $ds_i$ ,  $ds_{i_0}$  denote increments of arcs of the coordinate lines  $\xi^i$  at the current and initial moments of deformation (within each void being its linear dimensions):

$$ds_1 \approx \widehat{AA'}, ds_2 \approx \widehat{BB'}, ds_3 \approx \widehat{CC'}, ds_{1_0} \approx \widehat{A_0A'_0}, \dots \quad (\text{A.3})$$

In view of the relations (58) and (A.2) the relation (57) for the components  $\widehat{\varepsilon}_{ij}$  becomes:

$$\widehat{\varepsilon}_{ij} = \frac{1}{2} |\boldsymbol{\kappa}_{i_0}| |\boldsymbol{\kappa}_{j_0}| \left( \frac{ds_i}{ds_{i_0}} \frac{ds_j}{ds_{j_0}} \cos(\widehat{\psi}_k) - \cos(\widehat{\psi}_{k_0}) \right). \quad (\text{A.4})$$

If the accompanying coordinate system  $\xi^k$  of the initial state is Cartesian we have  $|\boldsymbol{\kappa}_{i_0}| = |\boldsymbol{\kappa}_{j_0}| = 1$ ,  $\cos(\widehat{\psi}_{k_0}) = \delta_{ij}$ , and the dependence (A.4) takes on the following form:

$$\widehat{\varepsilon}_{ij} = \frac{1}{2} \left( \frac{ds_i}{ds_{i_0}} \frac{ds_j}{ds_{j_0}} \cos(\widehat{\psi}_k) - \delta_{ij} \right), \quad (\text{A.5})$$

including the mixed components:

$$\begin{aligned} \widehat{\varepsilon}^{i \cdot j} &= \widehat{\varepsilon}_{kj} g^{ki} \\ &= \frac{1}{2} \left( \frac{ds_i}{ds_{i_0}} \frac{ds_j}{ds_{j_0}} \cos(\widehat{\psi}_k) - \delta_{ij} \right) \frac{1}{\left( \frac{ds_i}{ds_{i_0}} \right)^2} = \frac{1}{2} \left( \frac{ds_{i_0}}{ds_i} \frac{ds_j}{ds_{j_0}} \cos(\widehat{\psi}_k) - \delta_{ij} \left( \frac{ds_{i_0}}{ds_i} \right)^2 \right). \end{aligned} \quad (\text{A.6})$$

For example, in view of Eq. (A.3) all covariant components of the void strains can be found as:

$$\begin{aligned} \widehat{\varepsilon}_{11} &= \frac{1}{2} \left( \left( \frac{\widehat{AA'}}{\widehat{A_0A'_0}} \right)^2 - 1 \right), \quad \widehat{\varepsilon}_{12} = \frac{1}{2} \frac{\widehat{AA'} \widehat{BB'}}{\widehat{A_0A'_0} \widehat{B_0B'_0}} \cos(\widehat{\psi}_3), \\ \widehat{\varepsilon}_{13} &= \frac{1}{2} \frac{\widehat{AA'} \widehat{CC'}}{\widehat{A_0A'_0} \widehat{C_0C'_0}} \cos(\widehat{\psi}_2), \dots \end{aligned} \quad (\text{A.7})$$

## References

1. Armero, F., Oller, S.: A general framework for continuum damage models. I. Infinitesimal plastic damage models in stress space. *Int. J. Solids Struct.* **37**, 7409–7436 (2000)
2. Bernstein, M.L.: *Micro-structure of Deformed Metals*. Metallurgy, Moscow (1977) (in Russian)
3. Bogatov, A.A., Mizhiritskiy, O.I., Smirnov, S.V.: *Resource of Metals Plasticity during Forming*. Metallurgy, Moscow (1984) (in Russian)
4. Briottet, L., Klöcker, H., Montheillet, F.: Damage in a viscoplastic material. Part II. Overall behaviour. *Int. J. Plast.* **14**, 453–471 (1998)
5. Brunig, M.: An anisotropic ductile damage model based on irreversible thermodynamics. *Int. J. Plast.* **19**, 1679–1713 (2003)
6. Butuc, M.C., Gracio, J.J., Baratada Rocha, A.: An experimental and theoretical analysis on the application of stress-based forming limit criterion. *Int. J. Mech. Sci.* **48**, 414–429 (2006)
7. Chen, B., Li, W.G., Peng, X.H.: A microvoid evolution law involving change of void shape and micro/macrosopic analysis for damaged materials. *J. Mater. Process. Technol.* **122**, 189–195 (2002)
8. Demir, I., Zbib, H.M.: A mesoscopic model for inelastic deformation and damage. *Int. J. Eng. Sci.* **39**, 1597–1615 (2001)
9. Dung, N.L.: Plasticity theory of ductile fracture by void growth and coalescence. *Forsch. Ingenieurw.* **58**, 135–140 (1992)
10. Fan, J., Zhang, J.: An endochronic constitutive equation for damaged materials. *Chin. Sci. (Ser. A)* **32**, 246–256 (1989)
11. Fleck, N.A., Hutchinson, J.W.: Void growth in shear. *Proc. R. Soc. Lond. Ser. A* **407**, 435–458 (1986)
12. Gelin, J.C.: Modelling of damage in metal forming processes. *J. Mater. Process. Technol.* **80–81**, 24–32 (1998)
13. Glazoff, M.V., Barlat, F., Weiland, H.: Continuum physics of phase and defect microstructures: bridging the gap between physical metallurgy and plasticity of aluminum alloys. *Int. J. Plast.* **20**, 363–402 (2004)
14. Gurson, L.: Continuum theory of ductile rupture by void nucleation and growth. *J. Eng. Mater. Technol. Trans. ASME* **99**, 2–15 (1977)
15. Hill, R.: *The mathematical theory of plasticity*. Clarendon Press, Oxford (1983)
16. Horstemeyer, M.F., Matalanis, M.M., Sieber, A.M., Botos, M.L.: Micromechanical finite element calculations of temperature and void configuration effects on void growth and coalescence. *Int. J. Plast.* **16**, 979–1015 (2000)
17. Il'iusin, A.A.: *Plasticity: Fundamentals of the General Mathematical Theory*. Nauka, Moscow (1963) (in Russian)
18. Kachanov, L.M.: *Introduction to Continuum Damage Mechanics*. Kluwer, Dordrecht (1986)
19. Khraishi, T.A., Khaleel, M.A., Zbib, H.M.: A parametric-experimental study of void growth in superplastic deformation. *Int. J. Plast.* **17**, 297–315 (2001)
20. Klöcker, H., Tvergaard, V.: Growth and coalescence of non-spherical voids in metals deformed at elevated temperature. *Int. J. Mech. Sci.* **45**, 1283–1308 (2003)
21. Kolmogorov, V.L., Bogatov, A.A., Migachev, B.A.: *Plasticity and Fracture*. Metallurgy, Moscow (1977) (in Russian)
22. Korn, G.A., Korn, T.M.: *Mathematical Handbook for Scientists and Engineers: Definitions, Theorems, and Formulas for Reference and Review*. 2nd revised edn. Dover Publications, New York (2000)
23. Krajcinovic, D.: Damage mechanics: accomplishments, trends and needs. *Int. J. Solids Struct.* **37**, 267–277 (2000)
24. Lemaitre, J., Desmorat, R., Sauzay, M.: Anisotropic damage law of evolution. *Eur. J. Mech. A/Solids* **19**, 187–208 (2000)
25. Maire, E., Bordreuil, C., Babout, L., Boyer, J.-C.: Damage initiation and growth in metals. Comparison between modelling and tomography experiments. *J. Mech. Phys. Solids* **53**, 2411–2434 (2005)
26. Makarov, E.S., Tutyshkin, N.D., Gvozdev, A.E., Tregubov, V.I., Zapara, M.A.: *Technological Mechanics of Dilating Materials*. 3rd rev. and add. edn. Tul'skiy Polygraphist Publ., Tula (2007) (in Russian)
27. McClintock, F.A.: A criterion for ductile fracture by the growth of holes. *J. Appl. Mech.* **90**, 363–371 (1968)
28. Menzel, A., Steinmann, P.: A theoretical and computational framework for anisotropic continuum damage mechanics at large strains. *Int. J. Solids Struct.* **38**, 9505–9523 (2001)
29. Panin, V.E.: *Physical Mesomechanics of Heterogeneous Media and Computer-Aided Design of Materials*. Cambridge Publishing, Cambridge (1998)
30. Pironi, A., Bonora, N., Steglich, D., Brocks, W., Hellmann, D.: Simulation of failure under cyclic plastic loading by damage models. *Int. J. Plast.* **22**, 2146–2170 (2006)
31. Rice, J., Tracey, D.: On ductile enlargement of voids in triaxial stress field. *J. Mech. Phys. Solids* **17**, 201–217 (1969)
32. Sedov, L.I.: *Continuum Mechanics*, vol. 1. Nauka, Moscow (1983) (in Russian)
33. Tang, C.Y., Shen, W., Lee, T.C.: A damage-based criterion for fracture prediction in metal forming processes: a case study in Al 2024T3 sheet. *J. Mater. Process. Technol.* **89–90**, 79–83 (1999)
34. Thomson, C.I.A., Worswick, M.J., Pilkey, A.K., Lloyd, D.J.: Void coalescence within periodic clusters of particles. *J. Mech. Phys. Solids* **51**, 127–146 (2003)
35. Tutyshkin, N.D., Zapara, M.A.: The advanced method of definition of stress and velocity fields in the processes of axisymmetric plastic yielding. In: *WSEAS Trans. on Heat and Mass Transfer* vol. 2, pp. 150–156
36. Tutyshkin, N.D., Gvozdev, A.E., Tregubov, V.I.: *Complex Problems of Plasticity Theory*. Tul'skiy Polygraphist Publ., Tula (2001) (in Russian)
37. Voyiadjis, G.Z., Venson, A.R., Kattan, P.I.: Experimental determination of damage parameters in uniaxially-loaded metal-matrix composites using the overall approach. *Int. J. Plast.* **11**, 895–926 (1995)
38. Weinberg, K., Mota, A., Ortiz, M.: A variational constitutive model for porous metal plasticity. *Int. J. Comput. Mech.* **37**, 142–152 (2006)
39. Xiang, Y., Wu, S.: Numerical simulation of cavity damage evolution in superplastic bulging process. *J. Mater. Process. Technol.* **116**, 224–230 (2001)
40. Yokobori, T.: *An Interdisciplinary Approach to Fracture and Strength of Solids*. Wolters-Noordhoff Scientific Publications Ltd., Groningen (1966)
41. Zaikov, M.A.: Strength of carbon steels at high temperatures. *J. Tech. Phys.* **19**, 684–695 (1949) (in Russian)
42. Zhu, M., Jin, Q.L.: A constitutive relation for materials containing voids and application in closing of voids. In: Fan, J., Murakami, S. (eds.) *Proceedings of the ICCLEM, Chongqing*, pp. 542–545 (1989)